Electronics and Electrical Engineering

https://www.aimspress.com/journal/ElectrEng

AIMS Electronics and Electrical Engineering, 9(1): 46–59.
DOI: 10.3934/electreng.2025003
Received: 03 September 2024
Revised: 24 November 2024
Accepted: 13 December 2024
Published: 03 January 2025

Research article

Current-sensorless robust sliding mode control for the DC-DC boost converter

Said Oucheriah and Abul Azad*

Department of Engineering Technology, Northern Illinois University, DeKalb, Il 60115, USA

* **Correspondence:** Email: aazad@niu.edu.

Abstract: A current-sensorless PWM-based robust sliding mode controller is proposed for the DC-DC Boost Converter, a nonminimum phase system that presents major challenges in the design of stabilizing controllers. The development of the controller requires the measurement of the output voltage and the estimation of its derivative. An extended state observer is developed to estimate a lumped uncertainty that comprises the uncertain load and input voltage, the converter parasitics, and the component uncertainties, and also to estimate the derivative of the output voltage. A linear sliding surface is used to derive the controller that is simple in its design and yet exhibits excellent features in terms of robustness to external disturbances, parameter uncertainties, and parasitics, despite the absence of the inductor current feedback. Also, a simple procedure to select the controller gains is outlined. The robustness of the controller is validated by computer simulations.

Keywords: robust sliding mode control; DC-DC boost converter; current-sensorless control; extended state observer

1. Introduction

Sliding mode control (SMC) is a powerful nonlinear control strategy for DC-DC converters due to their variable structured nature. It offers several advantages, such as fast dynamic response, robustness to large parameter uncertainties and external disturbances, order reduction and ease of implementation. Despite these advantages, some traditional SMC, suffer from excessive chattering and require several sensors for their implementation. DC-DC converters are subject to external disturbances, parameter uncertainties and parasitics that must be taken into account in the design of robust controllers to tightly track the output reference voltage with minimum chattering and a reduction of the number of sensors. This is usually accomplished with the use of SMC in conjunction with a disturbance estimator. In most studies, the knowledge of the inductor current is required for the implementation of the controllers. The measurement of the inductor current can present challenges in the presence of noise and external

disturbances. Recently, there has been an interest in the use of current-sensorless controllers to reduce the cost and to improve the reliability and miniaturization of the device.

In the context of the DC-DC buck converter, some current-sensorless controllers were considered in [1–5]. For DC-DC boost converters, the design of stabilizing controllers based only on the output voltage measurement is a challenging task since the boost converter is bilinear in nature and a nonminimum phase system. The study in [6] proposes a unified nonlinear observer to estimate the inductor current of six different types of DC-DC converters. However, the observer developed relies on the knowledge of the values of the parasitics of the converter and also on the the input voltage measurement. Its effectiveness is validated both in simulation and experimental tests on converters subject to unknown load variations, and reference step changes only. In [7], a sliding mode controller is proposed that uses a state and disturbance observer (SDO) to estimate the inductor current in the presence of an unknown load. The input voltage is assumed to be known. The only parasitic considered is the inductor resistance that must be known for the implementation of the SDO and the controller. In [8], a nonlinear fast terminal sliding mode control is proposed for a two-phase interleaved boost converter. As in [7], the inductor resistance is assumed to be known for the implementation of the SDO and the controller. The authors assume that the load resistance and the input voltage are unknown. However, the input voltage and not its estimate appears in the expressions of the SDO and the controller. Using the nominal value of the input voltage may lead to an unsatisfactory response when the input voltage changes. In [7] and [8], other parasitics like the MOSFET on-resistance, the diode forward resistance, the conducting voltage of the diode and the capacitor equivalent series resistance with the parameter uncertainties of the converter were not accounted for in the design of their controllers. Also in practice, the values of the parasitics are unknown and must be estimated as part of an uncertain lumped signal.

In [9, 10], the immersion and invariance technique is employed to estimate the input voltage and inductor current using output voltage and control signal information. However, the robustness of the controllers developed was not tested against parasitics and parameter uncertainties of the converters. In [11], a finite-time generalized parameter estimation-based observer is adopted to estimate the inductor current of a boost converter with a PI passivity-based control to stabilize it. The robustness of the controller was simulated only for a load step change and its robustness to input voltage variation, parameter uncertainties and parasitics was not tested. In [12], a multiloop solution is developed for the output regulation of the DC-DC converter that utilizes an output voltage-derivative observer instead of the inductor current measurement. The tuning of the controller parameters is laborious, with many steps involved in the control scheme.

The effectiveness and performance of the controller on the output response of the converter depend on an accurate modeling of the system. Ignoring parasitics, parameter uncertainties, input voltage, and output load resistance disturbances in the design of the controller may result in a degradation of the output response. In this case, the output response may suffer from substantial steady-state errors with large output variations when the converters are subjected to large unknown time-varying external disturbances that may even lead to instability.

In this work, a current-sensorless robust sliding mode controller for the DC-DC boost converter is proposed. The derivative of the output voltage is estimated and used in the controller feedback instead of the measured inductor current. An extended state estimator is developed to estimate a lumped disturbance signal that includes load and input variations, parameter uncertainties and parasitics of

the converter and also to estimate the derivative of the output voltage. A linear sliding surface is used to derive the controller. The salient feature of this work is the simplicity of the design of the controller, with a very simple procedure to select the parameters of the sliding mode controller that is capable of dynamically compensating for the disturbance to achieve a high performance in terms of disturbance rejection despite the absence of the inductor current feedback. The robustness of the proposed controller is validated using simulations.

2. Current-sensorless robust sliding mode control design

2.1. DC-DC boost converter averaged model

A basic boost converter with parasitic elements is shown in Figure 1.

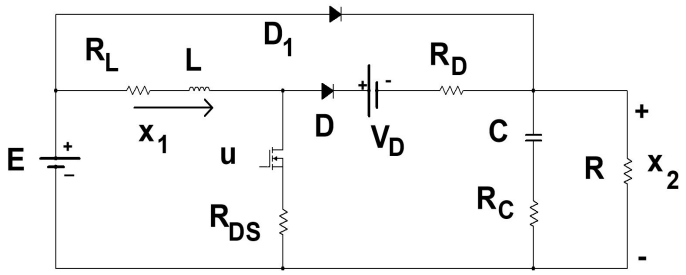

Figure 1. The boost converter.

Under continuous conduction mode (CCM), the averaged model of the boost converter is derived using Kirchhoff circuit laws in both modes, u = 1 (ON-state) and u = 0 (OFF-state) and then using the state-space averaging technique to obtain

$$\begin{aligned} \dot{x}_1 &= -\left(\frac{R_L}{L} + \frac{R_{DS}}{L}u + (1-u)\frac{R_D}{L}\right)x_1 \\ &\quad -(1-u)\frac{x_2}{L} - (1-u)\frac{V_D}{L} + \frac{E}{L} \\ \dot{x}_2 &= (1-u)\frac{x_1}{C} - \frac{x_2}{RC} + (1-u)R_C\dot{x}_1 - \frac{R_C}{R}\dot{x}_2 \end{aligned} \tag{2.1}$$

where x_1 represents the average inductor current, and x_2 is the output voltage across the load resistor. The unknown parameters E, L, C and R represent the input voltage, the inductance, the capacitance and the load resistance, respectively. However, their respective nominal values E_o, L_o, C_0 and R_o are assumed known for the implementation of the controller. The control input u to the converter is the duty ratio function. The unknown parameters R_L, R_{DS}, R_D, V_D and R_C represent the inductor equivalent series resistance, the MOSFET on-resistance, the diode forward resistance, the conducting voltage of the diode and the capacitor equivalent series resistance, respectively. The switching losses could have been accounted for by including a switching loss resistance in the inductor branch as proposed in [13]. In [14], a similar model with parasitics was considered with the diode D_1 and the diode forward resistance R_D of diode D missing. The average model uses the voltage across the capacitor C as a state variable instead of the true output voltage across the load resistor.

The complementary diode D_1 is added to improve the start-up of the converter [15, 16] and

guarantees that the initial condition of the capacitor voltage neglecting the parasitics is

$$x_2(0) = E \tag{2.2}$$

System (2.1) can be written as

$$\begin{aligned} \dot{x}_1 &= -(1-u)\frac{x_2}{L_o} + \frac{E_o}{L_o} + d_1 \\ \dot{x}_2 &= (1-u)\frac{x_1}{C_o} - \frac{x_2}{R_o C_o} + d_2 \end{aligned} \tag{2.3}$$

where

$$\begin{aligned} d_1 = &-\left(\frac{R_L}{L} + \frac{R_{DS}}{L}u + (1-u)\frac{R_D}{L}\right)x_1 - (1-u)\frac{V_D}{L} \\ &+(1-u)\left(\frac{1}{L_o} - \frac{1}{L}\right)x_2 + \left(\frac{E}{L} - \frac{E_o}{L_o}\right) \\ d_2 = &-\frac{R_C}{R}\dot{x}_2 + (1-u)R_C\dot{x}_1 + (1-u)\left(\frac{1}{C} - \frac{1}{C_o}\right)x_1 \\ &+\left(\frac{1}{R_o C_o} - \frac{1}{RC}\right)x_2 \end{aligned} \tag{2.4}$$

Taking the derivative of both sides of the second equation of (2.3) and using the expression for $\dot{x}_1$ given by the first equation of (2.3) yields

$$\ddot{x}_2 = (1-u)\frac{\dot{x}_1}{C_o} - \dot{u}\frac{x_1}{C_o} - \frac{\dot{x}_2}{R_o C_o} + \dot{d}_2$$

$$\begin{aligned} &= \frac{(1-u)}{C_o}\left[-(1-u)\frac{x_2}{L_o} + \frac{E_o}{L_o} + d_1\right] \\ &\quad -\dot{u}\frac{x_1}{C_o} - \frac{\dot{x}_2}{R_o C_o} + \dot{d}_2 \end{aligned} \tag{2.5}$$

$$\begin{aligned} &= -(1-u)^2\frac{x_2}{L_o C_o} + (1-u)\frac{E_o}{L_o C_o} + (1-u)\frac{d_1}{C_o} \\ &\quad -\dot{u}\frac{x_1}{C_o} - \frac{\dot{x}_2}{R_o C_o} + \dot{d}_2 \end{aligned}$$

The system (2.5) can be rewritten as

$$\ddot{x}_2 = \frac{2u}{L_o C_o}x_2 - \frac{uE_o}{L_o C_o} - \frac{\dot{x}_2}{R_o C_o} + d \tag{2.6}$$

where

$$\begin{aligned} d = &-\frac{u^2}{L_o C_o}x_2 - \frac{1}{L_o C_o}x_2 + \frac{E_o}{L_o C_o} - \dot{u}\frac{x_1}{C_o} \\ &+\frac{(1-u)}{C_o}d_1 + \dot{d}_2 \end{aligned} \tag{2.7}$$

Let

$$\begin{aligned} e_2 &= x_2 - V_{ref} \\ e_1 &= \dot{e}_2 \end{aligned} \tag{2.8}$$

Using the substitution $x_2 = e_2 + V_{ref}$, $\dot{x}_2 = e_1$ and $\ddot{x}_2 = \dot{e}_1$ into (2.6), model (2.1) can be redefined as

$$\begin{aligned} \dot{e}_1 &= \frac{u}{L_o C_o}\Big[2(e_2 + V_{ref}) - E_o\Big] - \frac{1}{R_o C_o} e_1 + d \\ \dot{e}_2 &= e_1 \end{aligned} \tag{2.9}$$

2.2. Design of the extended state observer

By using the lumped uncertainty d as a state variable, the extended state observer (ESO) for the system (2.9) is

$$\begin{aligned} \dot{\hat{e}}_1 &= \frac{u}{L_o C_o}\Big[2(e_2 + V_{ref}) - E_o\Big] - \frac{1}{R_o C_o}\hat{e}_1 + \hat{d} + K_1\tilde{e}_1 \\ \dot{\hat{e}}_2 &= \hat{e}_1 + K_2\tilde{e}_2 \\ \dot{\hat{d}} &= K_3\tilde{e}_1 \end{aligned} \tag{2.10}$$

where $\hat{e}_1, \hat{e}_2$ and $\hat{d}$ are the estimates of e_1, e_2 and d, respectively, and $\tilde{e}_1 = e_1 - \hat{e}_1$, $\tilde{e}_2 = e_2 - \hat{e}_2$. The parameters K_1, K_2 and K_3 are the observer gains. Please note that $\tilde{e}_1$ is used instead of $\tilde{e}_2$ in the third equation of (2.10) to estimate the lumped disturbance d. The error $\tilde{e}_1$ is very sensitive to external disturbances, especially to input voltage changes, and therefore, its use will in general require a smaller gain K_3. This will lead to less oscillatory responses during external disturbances than using $\tilde{e}_2$.

The extended state estimator (2.10) cannot be implemented because e_1 is not measured. It can be written as

$$\begin{aligned} \dot{\hat{e}}_1 - K_1 e_1 &= \frac{u}{L_o C_o}\Big[2(e_2 + V_{ref}) - E_o\Big] - \frac{1}{R_o C_o}\hat{e}_1 \\ &\quad + \hat{d} - K_1\hat{e}_1 \\ \dot{\hat{e}}_2 &= \hat{e}_1 + K_2\tilde{e}_2 \\ \dot{\hat{d}} - K_3 e_1 &= -K_3\hat{e}_1 \end{aligned} \tag{2.11}$$

Realizing that $\dot{e}_2 = e_1$, it is apparent that the auxiliary state variables q_1, q_2 and q_3 can be chosen as

$$q_1 = \hat{e}_1 - K_1 e_2,\ q_2 = \hat{e}_2,\ q_3 = \hat{d} - K_3 e_2 \tag{2.12}$$

and their use in (2.11) yields the following extended state estimator.

$$\begin{aligned} \dot{q}_1 &= \frac{u}{L_o C_o}\Big[2(e_2 + V_{ref}) - E_o\Big] - \frac{1}{R_o C_o}(q_1 + K_1 e_2) \\ &\quad + q_3 + K_3 e_2 - K_1 q_1 - K_1^2 e_2 \\ \dot{q}_2 &= q_1 + K_1 e_2 + K_2\tilde{q}_2 \\ \dot{q}_3 &= -K_3 q_1 - K_1 K_3 e_2 \\ \hat{e}_1 &= q_1 + K_1 e_2,\ \hat{e}_2 = q_2, \hat{d} = q_3 + K_3 e_2,\ \tilde{q}_2 = e_2 - q_2 \end{aligned} \tag{2.13}$$

Using (2.9) and (2.13), the dynamics of the state errors are

$$\begin{array}{l} \dot{\tilde{e}}_1 = -\left(\dfrac{1}{R_o C_o} + K_1\right)\tilde{e}_1 + \tilde{d} \\ \dot{\tilde{e}}_2 = \tilde{e}_1 - K_2\tilde{e}_2 \\ \dot{\tilde{d}} = -K_3\tilde{e}_1 + \dot{d} \end{array} \tag{2.14}$$

which can be written in a compact form as

$$\dot{\tilde{e}} = A\tilde{e} + B\dot{d} \tag{2.15}$$

where $\tilde{d} = d - \hat{d},\ \tilde{e} = [\tilde{e}_1,\ \tilde{e}_2,\ \tilde{d}]^T$ and

$$A = \begin{bmatrix} -\frac{1}{R_o C_o} - K_1 & 0 & 1 \\ 1 & -K_2 & 0 \\ -K_3 & 0 & 0 \end{bmatrix},\ B = \begin{bmatrix} 0 \\ 0 \\ 1 \end{bmatrix} \tag{2.16}$$

The eigenvalues of the system matrix A are determined from the characteristic equation

$$\begin{array}{c} s^3 + \left(\frac{1}{R_o C_o} + K_1 + K_2\right)s^2 + \left(\frac{K_2}{R_o C_o} + K_1 K_2 + K_3\right)s \\ +K_2 K_3 = 0 \end{array} \tag{2.17}$$

There always exist K_1, K_2 and K_3 such that the poles are on the left-hand side of the complex plane with the matrix A being Hurwitz. In this case, for any matrix $Q = Q^T > 0$, there exists a unique solution $P = P^T > 0$ satisfying the Lyapunov equation

$$A^T P + PA = -Q \tag{2.18}$$

Consider the Lyapunov function

$$V(\tilde{e}) = \tilde{e}^T P \tilde{e} \tag{2.19}$$

Its derivative along the solutions of (2.15) yields

$$\begin{array}{c} \dot{V} = -\tilde{e}^T Q\tilde{e} + 2\tilde{e}^T PB\dot{d} \\ \leq -\lambda_{min} Q\|\tilde{e}\|^2 + 2\|P\|\|B\|\|\tilde{e}\|\delta_1 \end{array} \tag{2.20}$$

and the observer estimation error $\tilde{e}$ is bounded by ϵ given by

$$\|\tilde{e}\| \leq \epsilon = 2\frac{\|P\|\delta_1}{\lambda_{min}(Q)} \tag{2.21}$$

where $\delta_1 = \sup_{t\in[0\ \infty)} \|\dot{d}\|$ and $\lambda_{min}(Q)$ denotes the minimum eigenvalue of Q.

2.3. Design of the controller and stability analysis

We consider the following sliding surface:

$$\begin{array}{c} \sigma = \hat{e}_1 + \gamma\hat{e}_2 - K_1 e_2 \\ = q_1 + \gamma q_2 \end{array} \tag{2.22}$$

where we have used $\hat{e}_1 = q_1 + K_1 e_2$ and $q_2 = \hat{e}_2$ and $\gamma > 0$ is a design parameter. We consider the following controller

$$\begin{aligned} u = \alpha\left(\tfrac{1}{R_o C_o} + K_1 - \gamma\right) q_1 - \alpha q_3 \\ +\alpha\left(\tfrac{K_1}{R_o C_o} - K_3 + K_1^2 - \gamma K_1\right) e_2 - \alpha K_2 \gamma \tilde{q}_2 - \alpha K_4 \sigma \end{aligned} \tag{2.23}$$

where

$$\alpha = \frac{L_o C_o}{\left[2(e_2 + V_{ref}) - E_o\right]} \tag{2.24}$$

Using (2.22), the controller (2.23) is derived by differentiating σ with respect to time and setting $\dot{\sigma} = 0$. The last term $\alpha K_4 \sigma$ is added to ensure the sliding mode condition.

The substitution of the controller (2.23) into the derivative of (2.22) leads to

$$\dot{\sigma} = -K_4 \sigma \tag{2.25}$$

and therefore we have $\dot{\sigma}\sigma = -K_4 \sigma^2 < 0$, which ensures the sliding mode condition. Equation (2.25) admits as a solution

$$\sigma(t) = \sigma(0) e^{-K_4 t} \tag{2.26}$$

Using the initial conditions $q_1(0) = 0,\ q_2(0) = 0$ for the extended state estimator (2.13), yields $\sigma(0) = 0$ and in this case $\sigma(t) = 0$ for all $t \geq 0$ with the reaching phase completely eliminated.

Theorem 1: For the system (2.1) with the extended state estimator (2.13) and driven by the controller (2.23), the output voltage x_2 is uniformly convergent to a ball $\Omega(r)$ centered at V_{ref} with a radius r given by

$$r = \frac{(\gamma + 1)\,\epsilon}{\gamma - K_1} \tag{2.27}$$

with a decay rate $(\gamma - K_1)$. Here $\gamma > K_1$ and the parameter ϵ is defined in (2.21)

Proof: Substituting $(e_1 - \tilde{e}_1)$ for $\hat{e}_1,\ (e_2 - \tilde{e}_2)$ for $\hat{e}_2$ and $\sigma = 0$ in equation (2.22) and solving for e_1 yields

$$e_1 = -(\gamma - K_1) e_2 + \tilde{e}_1 + \gamma \tilde{e}_2 \tag{2.28}$$

Using $e_1 = \dot{x}_2$ and $e_2 = x_2 - V_{ref}$ into (2.28) yields the following dynamic equation:

$$\dot{x}_2 = -(\gamma - K_1)(x_2 - V_{ref}) + \tilde{e}_1 + \gamma \tilde{e}_2 \tag{2.29}$$

In view of (2.21), $\|\tilde{e}_1\| \leq \epsilon,\ \|\tilde{e}_2\| \leq \epsilon$ and the solution x_2 of (2.29) is bounded by

$$|x_2| \leq \left[V_{ref} + \frac{(\gamma + 1)\,\epsilon}{\gamma - K_1}\right]\left(1 - e^{-(\gamma - K_1)t}\right) \tag{2.30}$$

and consequently, x_2 is uniformly convergent to a ball centered at V_{ref} with a radius r given by (2.27) and a decay rate $(\gamma - K_1)$.

Remark 1: If the lumped uncertainty d is bounded and satisfies $lim_{t\to\infty}\dot{d} = 0$, then $\tilde{e}_1,\ \tilde{e}_2$ and $\tilde{d}$ converge asymptotically to 0 with x_2 exponentially converging to V_{ref} with a decay rate $(\gamma - K_1)$.

In some situations where we have only step load resistance and step input voltage changes then we may have $\dot{d} \approx 0$ long after the onset of the step changes.
In this case and in view of (2.1), (2.12)-(2.14) and (2.23), we have

$$\begin{gathered} lim_{t\to\infty} e_2(t) = 0,\ lim_{t\to\infty} q_1(t) = 0 \\ lim_{t\to\infty} q_3(t) = d,\ lim_{t\to\infty} x_2(t) = V_{ref} \\ limit_{t\to\infty} \dot{u}(t) = 0,\ lim_{t\to\infty} \tilde{q}_2(t) = 0 \end{gathered} \tag{2.31}$$

Using the second equation of (2.1) with $lim_{t\to\infty}\dot{x}_1(t) = 0$ and $lim_{t\to\infty}\dot{x}_2(t) = 0$ yields

$$lim_{t\to\infty} x_1(t) = \frac{V_{ref}}{R(1-u)} \tag{2.32}$$

Using (2.31) and (2.32), the uncertainty d_1 and the derivative $\dot{d}_2$ of the uncertainty d_2 given both by (2.4) converge to

$$\begin{gathered} lim_{t\to\infty} d_1(t) = -\left(\frac{R_L}{L} + \frac{R_{DS}}{L}u + (1-u)\frac{R_D}{L}\right)\frac{V_{ref}}{R(1-u)} \\ -(1-u)\frac{V_D}{L} + (1-u)\left(\frac{1}{L_o} - \frac{1}{L}\right)x_2 + \left(\frac{E}{L} - \frac{E_o}{L_o}\right) \end{gathered} \tag{2.33}$$

$$lim_{t\to\infty}\dot{d}_2(t) = 0$$

and finally, the lumped uncertainty d given in (2.7) converges to

$$\begin{gathered} lim_{t\to\infty} d(t) = -\frac{u^2}{L_o C_o}V_{ref} - \frac{1}{L_o C_o}V_{ref} + \frac{E_o}{L_o C_o} \\ +\frac{(1-u)}{C_o} lim_{t\to\infty} d_1 \end{gathered} \tag{2.34}$$

Using (2.31), the steady state of the controller given in Eq (2.23) reduces to

$$u = -\frac{L_o C_o}{(2V_{ref} - E_o)} lim_{t\to\infty} d(t) \tag{2.35}$$

The substitution of the steady state value of $d(t)$ given by (2.34) into (2.35) and using (2.33) yields the following quadratic equation in u

$$au^2 + bu + c = 0 \tag{2.36}$$

where

$$a = \frac{L_o}{L}(V_D + V_{ref})$$

$$b = \frac{L_o V_{ref}}{LR}(R_{DS} - R_D) - \frac{L_o}{L}(2V_D + 2V_{ref} - E) \tag{2.37}$$

$$c = \frac{L_o V_{ref}}{LR}(R_L + R_D) + \frac{L_o}{L}(V_D + V_{ref} - E)$$

whose feasible solution is

$$u = \frac{-b - \sqrt{(b^2 - 4ac)}}{2a} \tag{2.38}$$

Its substitution in (2.32) yields the bounded inductor current x_1. In the absence of parasitics

$$R_L = 0\ \Omega, R_{DS} = 0\ \Omega, V_D = 0\ V, R_D = 0\ \Omega, R_C = 0\ \Omega \tag{2.39}$$

the solution to (2.36) is

$$u = 1 - \frac{E}{V_{ref}} \tag{2.40}$$

In this case, $0 < u < 1$ with the steady state inductor current

$$x_1 = \frac{V_{ref}^2}{RE} \tag{2.41}$$

Remark 2: In view of (2.14) and (2.29), a possible general guideline for the choice of the controller and estimator gains is:
1) Choose $K_1 = \frac{0.1}{R_oC_o}$ where R_oC_o is the nominal time constant of the open-loop system.
2) Choose $\gamma = \frac{m}{R_oC_o}$ with $m \geq 20$.
3) Finally, choose the gains $K_2 = 10(\gamma - K_1)$ and $K_3 = 10(\gamma - K_1)$ to ensure that the extended observer has faster dynamics than the controlled feedback system.
4) Choose $K_4 = 1$.
5) If the performance is not adequate, increase m in step 2 and repeat.

Shown in Figure 2, is the block diagram of the proposed current-sensorless robust sliding mode controller.

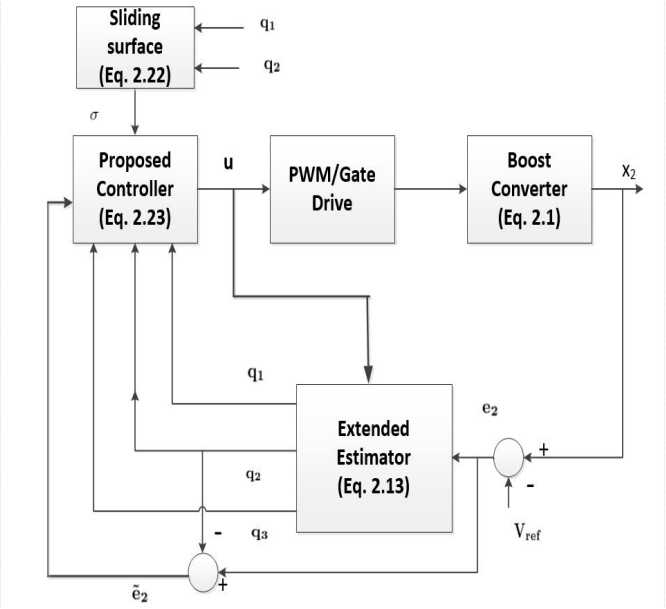

Figure 2. Block diagram of the proposed robust sliding mode controller.

3. Simulation results

The actual DC-DC boost converter parameters that are unknown to the designer are

$$E = 6\ V,\ L = 180\ \mu H,\ C = 250 \mu F,\ R = 40\ \Omega \tag{3.1}$$

To test the robustness of the proposed controller to the parameter uncertainties, the following nominal parameters that are known to the designer are used:

$$E_o = 9\ V,\ L_o = 90\ \mu H,\ C_o = 375\ \mu F,\ R_o = 48\ \Omega \tag{3.2}$$

The desired output voltage is $V_{ref} = 20\ V$. To account for the conduction losses, we consider the actual parasitics of the boost converter, which are unknown to the designer as

$$\begin{gathered} R_L = 0.2\ \Omega, R_{DS} = 0.01\ \Omega, V_D = 0.7\ V, R_D = 0.4\ \Omega \\ R_C = 0.1\ \Omega \end{gathered} \tag{3.3}$$

Using Remark 2 as a general guideline, the gains of the estimator/controller parameters are chosen as

$$\begin{gathered} K_1 = 5.56,\ \gamma = 19.44 \times 10^3,\ K_2 = 194.39 \times 10^3, \\ K_3 = 194.39 \times 10^3, K_4 = 1 \end{gathered} \tag{3.4}$$

with $m = 350$ and the initial conditions of the extended estimator $q_1(0) = 0, q_2(0) = 0$ and $q_3(0) = 0$.

Figure 3 depicts the time evolution of the output voltage x_2 due to load and input voltage changes. For the load disturbance rejection test, the converter is subject to a load step change from 40 Ω to 20 Ω at 0.2 s and from 20 Ω to 40 Ω at 0.4 s. The maximum voltage deviation is 2.5% and the disturbance is completely rejected in less than 50 ms. For the input voltage disturbance test, the converter is subject to a step input change from 6 V to 7 V at 0.6 s and from 7 V to 6 V at 0.8 s. The maximum voltage deviation is 4% and the disturbance is completely rejected in less than 50 ms. Figures 4, 5, 6 and 7 depict the inductor current x_1, the duty ratio u, the sliding surface σ and the actual disturbance d and its estimate $\hat{d}$, respectively. As seen in this simulation, the proposed controller exhibits an excellent disturbance suppression capability during load and input voltage changes with small overshoosts and short recovery times.

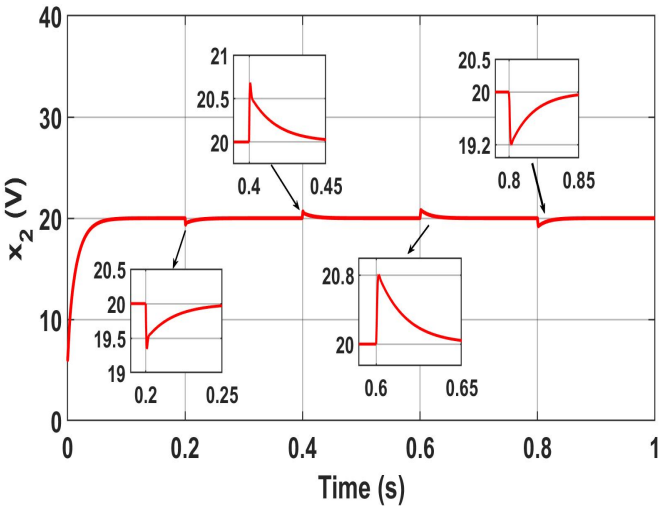

Figure 3. Output response due to load and input variation.

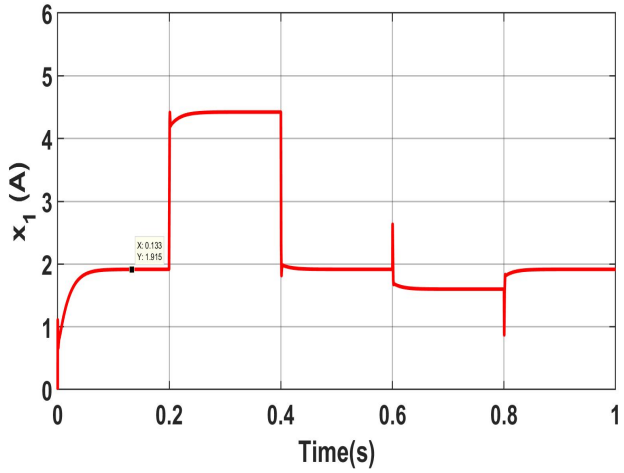

Figure 4. Inductor current.

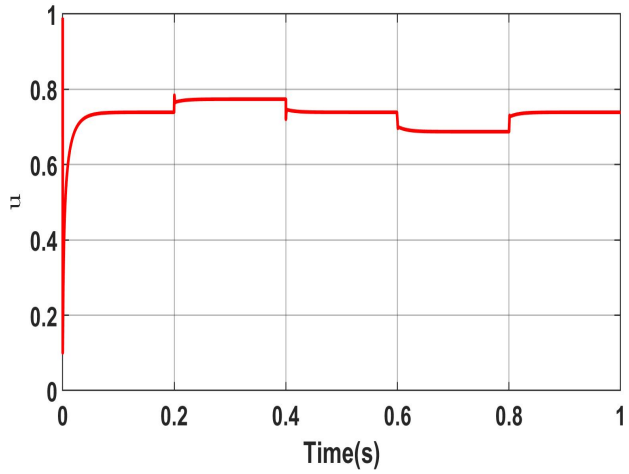

Figure 5. Duty ratio u.

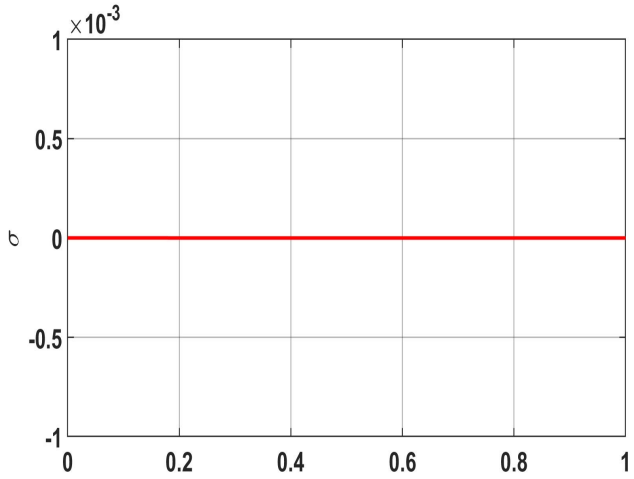

Figure 6. Sliding surface σ.

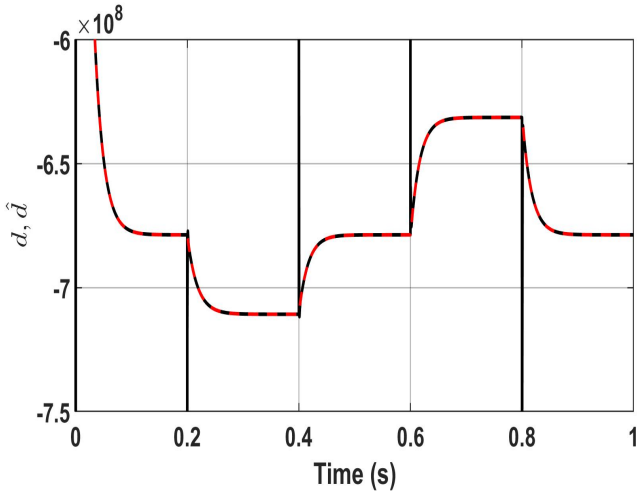

Figure 7. Actual disturbance d in black and its estimate $\hat{d}$ in red.

4. Conclusions

A PWM-based current-sensorless robust sliding mode controller for the DC-DC boost converter is proposed that requires only one sensor for the output voltage measurement. An extended state observer is used to estimate a lumped uncertainty signal that comprises the uncertain load and the input voltage, parameter uncertainties, parasitics and also to estimate the derivative of the output voltage. A linear sliding surface is used to derive the controller. The controller proposed is simple in its design and yet exhibits excellent features in terms of disturbance suppression despite the absence of the inductor current feedback. Its robustness is validated by computer simulations. Future work will be the validation of these results experimentally and the development of a systematic procedure to determine the gains of the controller to meet certain specifications.

Author contributions

Said Oucheriah: Conceptualization, methodology, software, validation, formal analysis, writing-original draft preparation. Abul Azad: Validation, writing-review and editing, supervision, project administration, funding acquisition. All authors have read and approved the final version of the manuscript.

Use of Generative-AI tools declaration

The authors declare they have not used Artificial Intelligence (AI) tools in the creation of this article.

Acknowledgments

We would like to express our sincere gratitude to the reviewers for their valuable comments and suggestions, which, in our opinion, have significantly enhanced the quality of this manuscript.

Conflict of interest

The authors declare no conflict of interest in this paper.

References

1. Pandey SK, Patil SL, Ginoya D, Chaskar UM, Phadke SB (2019) Robust control of mismatched buck DC-DC converters by PWM-based sliding mode control schemes. *Control Eng Pract* 84: 183–193. https://doi.org/10.1016/j.conengprac.2018.11.010
2. Zuo Wang S L, Jun Yang Q L (2018) Current sensorless finite-time control for buck converters with time-varying disturbances. *Control Eng Pract* 77: 127–137. https://doi.org/10.1016/j.conengprac.2018.05.014
3. Wang JX, Rong JY, Li Y (2021) Reduced-order extended state observer based event-triggered sliding mode control for DC-DC buck converter system with parameter perturbation. *Asian J Control* 23: 1591–1601. http://doi.org/10.1002/asjc.2301
4. Wang B, Li S, Kan S, Li J (2023) Enhanced tracking of DC-DC buck converter systems using reduced-order extended state observer-based model predictive control. *Int J Intell Syst* 2: 143–152. https://doi.org/10.56578/jisc020303
5. Oucheriah S (2024) Current-Sensorless Robust Sliding Mode Control for the DC-DC Buck Converter. *Preprint at Research Square.* https://doi.org/10.21203/rs.3.rs-4103291/v1
6. Cimini G, Ippoliti G, Orlando G, Longhi S, Miceli R (2017) A unified observer for robust sensorless control of DC-DC converters. *Control Eng Pract* 61: 21–27. https://doi.org/10.1016/j.conengprac.2017.01.012
7. Pandey SK, Patil SL, Chaskar UM, Phadke SB (2019) State and Disturbance Observer-Based Integral Sliding Mode Controlled Boost DC-DC Converters. *IEEE Trans Circuits Syst II Express Briefs* 66: 1567–1571. https://doi.org/10.1109/TCSII.2018.2888570
8. Malge SV, Patil SL, Chincholkar SH, Ghogare MG, Aher PK (2024) Inductor current estimation based sensorless control of boost type DC-DC converter. *Control Eng Pract* 153: 106119. https://doi.org/10.1016/j.conengprac.2024.106119
9. Malekzadeh M, Khosravi A, Tavan M (2019) A novel sensorless control scheme for DC-DC boost converter with global exponential stability. *Eur Phys J Plus* 134: 338. https://doi.org/10.1140/epjp/i2019-12664-4
10. Malekzadeh M, Khosravi A, Tavan M (2020) A novel adaptive output feedback control for DC-DC boost converter using immersion and invariance observer. *Evol Syst* 11: 707–715. https://doi.org/10.1007/s12530-019-09268-7
11. Zhang X, Martinez-Lopez M, He W, Shang Y, Jiang C, Moreno-Valenzuela J (2021) Sensorless Control for DC-DC Boost Converter via Generalized Parameter Estimation-Based Observer. *Appl Sci* 16: 7761. https://doi.org/10.3390/app11167761
12. Kim SK, Lee KB (2022) Current-Sensorless Energy-Shaping Output Voltage-Tracking Control for dc-dc Boost Converters With Damping Adaptation Mechanism. *IEEE Trans Power Electron* 37: 9266–9274. https://doi.org/10.1109/TPEL.2022.3159793

13. Ayachit A, Kazimierczuk MK (2019) Averaged Small-Signal Model of PWM DC-DC Converters in CCM Including Switching Power Loss. *IEEE Trans Circuits Syst II Express Briefs* 66: 262–266. https://doi.org/10.1109/TCSII.2018.2848623

14. Leon-Masich A, Valderrama-Blavi H, Bosque-Moncusi JM, Maixe-Altes J, Martinez-Salamero L (2015) Sliding-Mode-Control-Based Boost Converter for High-Voltage-Low-Power Applications. *IEEE Trans Ind Electron* 62: 229–237. https://doi.org/10.1109/TIE.2014.2327004

15. Martinez-Trevino BA, El Aroudi A, Valderrama-Blavi H, Cid-Pastor A, Vidal-Idiarte E, Martinez-Salamero L (2021) PWM Nonlinear Control With Load Power Estimation for Output Voltage Regulation of a Boost Converter With Constant Power Load. *IEEE Trans Power Electron* 36: 2143–2152. https://doi.org/10.1109/TPEL.2020.3008013

16. Zambrano-Prada D, El Aroudi A, Vazquez-Seiszdedos L, Lopez-Santos O, Haroun R, Martinez-Salamero L (2023) Adaptive Sliding Mode Control for a Boost Converter with Constant Power Load. *2023 IEEE Conference on Power Electronics and Renewable Energy (CPERE),* 1-6. https://doi.org/10.1109/CPERE56564.2023.10119573

AIMS Press